User-centric non-full interference cellular networks: BS cooperation and bandwidth partitioning

Mohammadreza Mardani, Philippe Mary, Jean-Yves Baudais

Mardani *et al. J Wireless Com Network* (2022) 2022:108
https://doi.org/10.1186/s13638-022-02189-1

EURASIP Journal on Wireless Communications and Networking

RESEARCH Open Access

User-centric non-full interference cellular networks: BS cooperation and bandwidth partitioning

Mohammadreza Mardani*, Philippe Mary and Jean-Yves Baudais

*Correspondence: mardani.vmz@gmail.com

Univ Rennes, INSA Rennes, CNRS, IETR-UMR 6164, Rennes, France

Abstract

This paper presents a user-centric frequency reuse scheme depending on the user classification in the cell in a homogeneous Poisson point process network. Each cell is partitioned into multiple regions delimited by the signal-to-interference ratio of the user considered. A given resource block (RB) is assigned to one user in a cell and cannot be shared by another user in this cell. The typical user only uses a fraction of the RB, and the remaining part is left unused to avoid interference with the other cells. The base stations (BS) interfering set is hence determined by the coverage probability of the typical user, and this set can be approximated by a thinned version of the original PPP. Using this, coverage probability and spectral efficiency (SE) for each user types are derived, and a BS cooperation technique is proposed to improve the SE of the cell edge user. Finally, the average network spectral efficiency and fairness among users are analyzed under the developed theoretical framework. Our results show that the user-centric frequency reuse improves the coverage probability and the SE compared to the conventional frequency reuse scheme.

Keywords: User classification, Bandwidth partitioning, Fixed-point equation, Coverage probability, Spectral efficiency, Poisson point process

1 Introduction

In interference-dominated downlink cellular networks, the quality of service depends on the relative signal strength received from the serving base station (BS) and all other interfering BS through the so-called signal-to-interference ratio (SIR), which in turn depends on the network geometry and channel conditions. In a conventional full interference network, where all BS are active all the time in the same band, users near the cell boundary are known to experience a low SIR [1]. However, in a non-full interference network, locating close to the cell edge does not necessarily lead to significant performance degradation. A non-full interference in downlink refers to the situation in which all BS do not contribute to the interference received by a user in a given bandwidth [2]. To help users who are more likely to be affected by interference, operators often divide available bandwidth into smaller frequency bands and use the frequency reuse technique to reduce the co-channel interference, by not allocating the same frequencies to

neighboring cells. This concept can be extended by categorizing users based on their locations into cell center users and cell edge users and then allocating different subbands to each [3]. However, the location-based user classification is a purely geometrical approach and ignores the user's SIR, which may be a useful metric for classifying users. The SIR is indeed used to know active BS distribution in a non-full interference network.

A generally used approach in the literature is to consider that the BS activity depends on the presence or not of users in a cell. If there is no user in a cell, the cell's BS is inactive [2]. Under this scenario, authors of [4] model the interference as a random thinning of the original Poisson point process (PPP) of BS, with an approximated empty cell probability. However, when all BS have users inside their cells, the activation of a BS should depend on whether the user is covered or not and hence on its SIR in the cell. From this viewpoint, a better criterion of BS activation could be obtained by correlating the activity of BS with its coverage region.

In this paper, the BS activity on a given band is conditioned on the SIR experienced by a user leading to the non-full interference concept. This definition strongly differs from the classical frequency reuse concept which is widely used, in the sense that the interference created by a BS on a given band depends on the coverage probability of the tagged user. This dependency makes the analysis of the coverage probability or average spectral efficiency (SE) rather involved since the considered metric depends on itself. Indeed, in this model, which will be detailed in Sect. 2, users are classified according to their SIR with respect to predefined thresholds. A resource block (RB) is allocated to each user class, but a user in a certain class is allowed to use only a fraction of the RB and let the remaining band of RB free that can be used only by the other kind of users in the neighboring cell. This concept naturally leads to a user-centric frequency reuse scheme. We show that the user classification within each cell drives the BS activity. This is because the density of interfering BS for each user type is correlated with the type of the user. We present an analytical framework based on stochastic geometry to cope with the spatial distribution of different types of users. This analytical framework allows quantifying key performance measures, i.e., coverage probability and SE, in the non-full interference context. Moreover, a BS cooperation technique under the introduced non-full interference framework is studied to improve the SE of cell edge users without jeopardizing the other scheduled users in the same RB. Finally, a bandwidth allocation among users by considering trade-off on the average SE of the network and the fairness for all user types is proposed and compared with different bandwidth allocation scenarios. In the following, literature related to the main topics of this paper is reviewed: classification of users, BS cooperation and bandwidth partitioning.

1.1 Related work

1.1.1 User classification

Stochastic geometry is a powerful tool to link the performance of users to their location, which implies user classification in large-scale cellular networks [3]. However, combining sophisticated user classification methods based on the link qualities and inter-cell interference is challenging [5]. It is because of the correlation between the received signal and the inter-cell interference seen by the users in the network. Therefore, most of the existing studies in the literature ignore this correlation and instead

sort the users according to their mean desired signal strength (i.e., link distances) such that the kth nearest user is the kth strongest user [6]. In the open literature, user classification schemes mainly focus on distance-based [2, 3, 5, 7–9], and SIR-based classification [10–12].

For instance, in [5, 7, 8], the ratio of the distance between the typical user and the serving BS to the distance between the typical user and the nearest interfering BS is computed. If the ratio is larger than a threshold, the user is a cell edge user; otherwise, it is a cell center user. Authors in [5] studied a meta-distribution of the cell center/edge user under orthogonal and non-orthogonal multiple access. A similar approach for classifying users is also used at 3GPP to analyze the performance of schemes such as soft frequency reuse (SFR) [13]. Inspired by this, base station cooperation techniques have been investigated to enhance the cell edge user's coverage [2, 3, 9]. However, this approach for incorporating a user as a cell center/edge user is not proper for the next-generation cellular networks because of neglecting the effects of fading channel and inter-cell interference seen by the users, which can make them experience low coverage performance even in the cell center area [14].

The SIR ratio is a more suitable way for classifying the users [10, 11]. In [10], the entire frequency band has been split into two sub-bands that are used to separate cell center and cell edge users. Moreover, spectrum access strategies such as fractional and soft frequency reuse are proposed to increase the cell edge user's coverage. In [11], the authors used the instantaneous signal-to-noise-plus-interference ratio to classify users and got an approximation of the coverage probability of the typical cell edge user for a PPP-modeled 3-tier heterogeneous network. However, since all BS are active in the classical full interference scenario, both aspects, geometrical-based and SIR-based classifications, lead to similar conclusions on average, and a user located at the cell border undergoes severe performance degradation.

Indeed, in all previous works, full interference in a given resource block is implicitly assumed. Even in the case of frequency reuse or SFR, in a given frequency band all BS are assumed to transmit (and hence creating interference) independently of the status, covered or not, of their users. These works ignore the correlation in the BS activity, which is a function of the randomly selected user in the cell in the scheduled resource.

In our previous work [12], an SIR-dependent non-full interference model has been introduced to address the existing analytical models' shortcoming. In our model, the given RB is assigned to a single user in each cell and cannot be shared within the cell. With two user types, the RB is thus divided into two sub-bands, each being used exclusively depending on whether the user is a cell center or cell edge user, with a portion of the RB remaining unused to reduce interference to the other cell. This work has been extended to N user classes, and the key performance metrics, i.e., the coverage probability and the SE, in a non-full interference context, have been addressed in [15]. It has been found that these metrics are the solution of fixed-point equations. However, cell edge users still suffer from performance degradation and cooperation techniques to improve their performance have not been studied in the context of non-full interference network. Moreover, the fairness induced by the user-centric frequency reuse approach has not been tackled neither.

1.1.2 BS cooperation

The analysis of the performance enhancement of a typical user based on BS cooperation in cellular networks using stochastic geometry has been investigated in several works [2, 3, 16–19]. In [2], a semi-closed-form expression for the typical edge user's coverage probability has been obtained. It is assumed that each BS serving a cell center user and placed within the so-called cooperation radius from an edge user cooperates and does not transmit any signal at the tagged time slot. A user-centric BS cooperation scheme with the joint transmission has been analyzed in [3], where users are grouped by their relative received signal strengths to the three strongest BS. The typical edge user's performance in millimeter wave cellular networks under two cooperative schemes, namely fixed-number BS cooperation scheme and fixed-region BS cooperation scheme, has been investigated in [9]. A Poisson–Delaunay triangulation-based BS cooperation approach has been proposed to improve the cell edge users' performance in [20]. The authors of the work in [14] proposed a hybrid cooperation scheme for sub-6 GHz cellular networks where an edge user chooses its mode of operation with or without cooperation. According to the follow-up studies, BS cooperation was investigated for the typical link, which represents all other links in a full interference scenario. In these works, cooperating BS should abandon scheduled users in their cells by delaying them until the next round of transmissions which may increase the network traffic load.

In contrast, in the non-full interference network presented in this paper, each BS is allowed to transmit a signal to its served user in the assigned fraction of the scheduled RB, and it is off in the remaining subchannels of the RB. This technique hence allows a BS to help a neighboring cell edge user without postponing the service to its own user. Considering this scenario, an edge user can send a cooperation request to BS which serves different user types. In this paper, a cooperation technique, named optimal point selection (OPS), is applied to improve the cell edge user's performance under the non-full interference model. In OPS technique, data are concurrently available at multiple BS; only one BS out of the BS cooperation set sends data to a user [21, 22]. In our model, we aim at improving the performance of the cell edge user without jeopardizing other scheduled users in the same RB and without raising the interference level in the network. It is the opposite of the conventional approach in BS cooperation that focuses on a typical user and drops connected users in other cells to help the tagged typical user [2].

1.1.3 Bandwidth partitioning

Besides user classification and BS cooperation technique, bandwidth partitioning (BWP) is a part of the non-full interference network. Given existing challenges like restricted spectrum availability and poor spectrum usage, efficient radio resource usage is critical for reaching the high peak data rates. A full frequency reuse factor of one appears to be the most effective solution for meeting SE performance goals. However, BWP introduces a trade-off between radio resource utilization efficiency and interference management [23]. The authors in [24] proposed a bandwidth allocation model that is able to adapt bandwidth allocation to individual users based on data rate requirements. These analyses rely on precise representations of key performance metrics, such as the success

probability, signal-to-interference ratio and Shannon throughput. In [25], the author investigated the effect of BWP on the reliability and delay performance. Reliability is measured in terms of simultaneous transmission density that meets certain reliability constraints, whereas the delay is measured in terms of average number of time slots for successful transmission of a packet. On this line, prior works have investigated BWP for the downlink full interference system using various performance metrics, such as user fairness [26] and weighted sum-rate maximization [27]. In this paper, we investigate BWP for the non-full interference scenario where the interference received by users is correlated by their types in the network. Based on this model, we can quantify spectrum sharing and service differentiation in this particular context, namely what performance will be delivered to a user based on its type as well as overall performance. Assuming that an RB is partitioned into N parts, i.e., for N user types, we study different BWP strategies. A risk-averse BWP scheme considering trade-off on the average spectral efficiency of the network and the fairness for all user types is proposed and compared with different BWP strategies.

1.2 Contributions

The aim of this paper is to define edge users in cellular networks based on active neighbor BS and to propose a SIR-dependent user-centric frequency reuse scheme that improves the quality of service to the newly defined edge users. Specifically, this paper studies the non-full interference cellular networks from the perspective of stochastic geometry. As discussed in Section I–A, it is challenging to combine sophisticated user classification methods based on link qualities and inter-cell interference. Despite this, the related works do not explicitly classify users with distinct signal qualities, which is crucial to accurately detecting user performance degradation. This means that these analyses do not capture the correlation in the SIR induced by the fact that the user's interference set is a function of its coverage probability. The non-full interference model presented in this paper overcomes the above limitations while enabling the tractable system-level study of the typical user performance in downlink non-full interference networks using stochastic geometry. The contributions of our study are briefly summarized below.

- The activity of a BS within a cell is correlated with the user classification in our novel definition of a non-full interference network;
- An accurate approximation of the user classification probability is derived. This expression represents how the desired signal correlates with the interference set for each type of user using a fixed-point equation. Besides, we also provide per user type performance metrics, namely coverage probability and SE;
- This paper re-formulates OPS's cooperation theory in the framework of our proposed non-full interference cellular network model. In this way, cell edge users will experience improved performance without compromising the performance of other users;
- In order to formulate different methods of BWP, the user-centric frequency reuse model is used. As a network perspective, the objective is to maximize SE under constraints, while minimizing SE's variance to ensure fairness between types of users.

We propose a risk-averse BWP approach, inspired from the portfolio theory [28], to find a mean–variance trade-off for the network performance;

- Our numerical results demonstrate that: (*i*) in comparison with the conventional frequency reuse scheme, our user-centric frequency reuse boosts network efficiency and allows high SE, (*ii*) the non-full interference-based BS cooperation can help vulnerable users without penalizing other users in other cells, (*iii*) the proposed trade-off BWP strategy assigns fair shares to the different types of users based on their performance metrics.

The rest of this paper is organized as follows. Section 2 describes the system model and the principle of constructing the active BS sets. Section 3 briefly revisits our previous results on coverage and SE of a typical user in a non-full interference network. Section 4 is devoted to type N user performance enhancement using optimal point selection. Moreover, a modern portfolio theory-based model is applied to optimize the network SE considering BWP's fairness in Sect. 5. Simulation results are presented and discussed in Sect. 6. Finally, Sect. 7 concludes the paper.

1.2.1 Notations

Random variables are denoted in capital letters, while their realizations remain in lowercase. The operators $\mathbb{P}(\cdot)$ and $\mathbb{E}[\cdot]$ denote the probability and the mathematical expectation functions, $[\![n_1, n_2]\!]$ is the interval of all integers between n_1 and n_2, and $\mathbf{1}(\mathcal{P}) \in \{0, 1\}$ is the indicator function, which is one when the proposition $\mathcal{P}$ is true and is null otherwise. The Gamma function is defined as $\Gamma(a) \triangleq \int_0^\infty t^{a-1}e^{-t}\,\mathrm{d}t$ for all $a > 0$. The hypergeometric function is defined as ${}_2F_1(a, b; c; z) \triangleq \frac{\Gamma(c)}{\Gamma(b)\Gamma(c-b)} \int_0^1 t^{b-1}(1-t)^{c-b-1}(1-zt)^{-a}dt$, for $c > b > 0$ and $a > 0$ [29].

2 Methods and problem formulation

2.1 Network modeling

Let us consider an OFDMA-based single-tier downlink cellular network where the location of BS is modeled as an homogeneous PPP $\Phi \equiv \{X_1, X_2, ...\}$ with density λ and $X_i \in \mathbb{R}^2$. The given set of nucleus at $X_i \in \Phi$ can divide the space into Poisson–Voronoi regions as

$$V_i = \left\{ Y \in \mathbb{R}^2 : \|Y - X_i\| \leq \|Y - X_j\|, \forall j \neq i,\ X_j \in \Phi \right\}. \tag{1}$$

Similar to the works in [12, 30], the location of the users on a given RB is a point process such as $\Omega \triangleq \{U(V_i) : X_i \in \Phi\}$. Here, $U(B)$ is chosen uniformly at random from the set B independently for different B. Hence, only one randomly chosen user per RB is considered to communicate with its BS. Since by Slivnyak's theorem, conditioning on a point is the same as adding a point to the PPP, we consider that the nucleus of the typical cell of the point process $\Phi \cup \{X_0\}$ is located at X_0 with its typical cell V_0. Note that the typical user from the point process Ω describes a uniformly random point process in the typical cell.

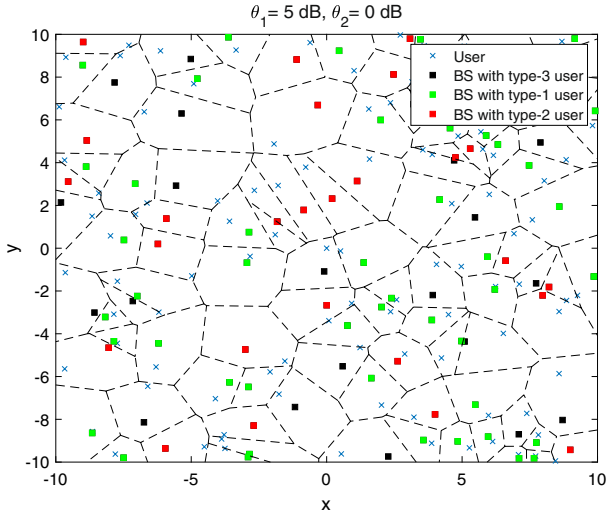

Fig. 1 PPP deployment for BS with a randomly selected user in each cell. Fig. 1 illustrates one realization of a PPP network for three types of served users, with only one user per BS represented by *X*. The BS colored in green, red and black represent the active BS for users of type 1, type 2 and type 3, respectively.

The standard power-law path loss model with exponent $\alpha > 2$ is considered for signal propagation. We assume that all BS and users are equipped with a single antenna, and users are experiencing an independent block Rayleigh fading channel on each RB. A cell is divided into N classes, and a typical user belongs to a certain class depending on its SIR. Moreover, each class has its proper sub-band that may be used by the nearest interfering cell but only by the same user type in that interfering cell. In our model, a user is classified to be a type 1 when its SIR on subchannel 1 is larger than a threshold; a user is type 2 if its SIR on subchannel 1 is less than the first-class threshold and its SIR on subchannel 2 is larger than the second class one, and so on. A type N user has all its SIR lower than the thresholds in all subchannels 1 to $N-1$ and may be in outage in the last remaining subchannel N. Contrary to the type N user, all type k users are covered with a probability equal to one (by definition). The type 1 user is a cell center user while the type N is the cell edge one. By the above construction, the typical user is a type k user according to the relative value of its SIR w.r.t. some thresholds that, in turn, depends on the location of others BS and the channel conditions. Figure 1 illustrates one realization of a PPP network for three user types, with only one user per BS in a given RB. The BS colored in green, red, and black represent the active BS for type 1, type 2, and type 3 users, respectively. The RB is allocated to all considered users within the network, one user in each cell. This feature can take advantage of 4G or 5G systems in which the RB is divided into multiple subcarriers. However and contrary to 4G, type k user uses only subchannel k although the entire RB is associated to this user. Since the entire RB is dedicated to a given type of user, the BS cannot allocate the remaining part of the RB to another user in the cell. This setting leads to a non-full interference context in each subchannel because only a part of the RB is used in a given cell. The other users in a cell are associated to other RB of the entire frequency band.

2.2 Proposed user—BS classification

Let us consider the typical BS at X_0 and divide the interfering BS set Φ into $N \geq 2$ complementary subsets $\{\Phi_k\}_{k=1}^N$ such that $\Phi = \cup_{k=1}^N \Phi_k$ and $\Phi_k \cap \Phi_l = \emptyset$ for all $k \neq l$. When $k \in [\![1, N-1]\!]$, Φ_k is the subset that gathers the BS serving type k users across the network such that BS in Φ_k fully cover their associated users. The BS in Φ_N are transmitting with the worse link quality, and they may have users in outage.

Let X_i be the position of BS i, and SIR_i^k be the SIR experienced by a randomly selected user in the cell i over the subchannel k. The subset Φ_k is

$$\Phi_k \triangleq \begin{cases} \left\{X_i \ : \ \mathrm{SIR}_i^k \geq \theta_k \text{ and } \mathrm{SIR}_i^m < \theta_m, \forall m,\ 1 \leq m < k\right\},\ 1 \leq k \leq N-1 \\ \left\{X_i \ : \ \mathrm{SIR}_i^m < \theta_m, \forall m,\ 1 \leq m < k\right\},\ k = N \end{cases}, \tag{2}$$

where $\theta_k > 0$, $\forall k \in [\![1, N]\!]$, are the SIR classification thresholds. For the subset Φ_N, the SIR_i^N can be higher or lower than the threshold θ_N. Let SIR_0^k be the received SIR by the typical user in V_0, on subchannel k, then

$$\mathrm{SIR}_0^k = \frac{H_0^k R_0^{-\alpha}}{\sum\limits_{X_i \in \Phi} H_i^k R_i^{-\alpha} \mathbf{1}(X_i \in \Phi_k)} = \frac{S_0}{I_{0,k}}, \tag{3}$$

where R_i is the distance between the BS i and the typical type k user, H_i^k is the channel gain between the typical user and the BS i in subchannel k. Since separated frequency sub-bands are allocated to different user types, they do not experience the same instantaneous channel gain, and H_i^k are independent and identically exponentially distributed (i.i.e.d.). The indicator function in (3) ensures that the typical user only experiences interference from BS that serve type k users.

3 Coverage and spectral efficiency without cooperation

This section first revisits the coverage probability of the typical user under a user-centric frequency reuse approach in the non-full interference network. Next, to fairly evaluate the proposed method, the SE of the network is studied.

3.1 Coverage probability

In interference-limited wireless networks, the standard coverage probability describes the probability that the SIR of the typical link exceeds a threshold [31]. In our model, we have a set of thresholds $\{\theta_k\}_{1 \leq k \leq N}$ to successfully demodulate and decode the received signal. Then, the typical user located in the typical cell is covered on downlink if:

$$X_0 \in \Phi_1 \cup \cdots \cup \Phi_{N-1} \cup \{\Phi_N, \mathrm{SIR}_0^N \geq \theta_N\}. \tag{4}$$

The following corollary presents the downlink coverage probability of the typical user for a non-full interference network with N classes.

Corollary 1 *Given* $\{\theta_k\}_{1\le k\le N}$*, the coverage probability of a randomly located typical user in a non-full interference network with N user types is given by*

$$\mathcal{P}_{\text{cov}}\left(\{\theta_k\}_{k=1}^{N},\alpha,\lambda\right)=\sum_{k=1}^{N-1}p_k+p_N\cdot\mathcal{P}_N\left(\{\theta_k\}_{k=1}^{N},\alpha,\lambda\right), \tag{5}$$

where

$$p_k=\int_0^{\infty}e^{-\nu(1+p_k\rho(\theta_k,\alpha))}\prod_{i=1}^{k-1}\left(1-e^{-p_i\rho(\theta_i,\alpha)\nu}\right)\mathrm{d}\nu\,,\ \forall\, k\in[\![1,N-1]\!] \tag{6}$$

$$p_N=1-\sum_{k=1}^{N-1}p_k, \tag{7}$$

$$\mathcal{P}_N\left(\{\theta_k\}_{k=1}^{N},\alpha,\lambda\right)=\frac{1}{p_N}\int_0^{\infty}e^{-\nu(1+p_N\rho(\theta_N,\alpha))}\prod_{i=1}^{N-1}\left(1-e^{-p_i\rho(\theta_i,\alpha)\nu}\right)\mathrm{d}\nu, \tag{8}$$

and

$$\rho(\theta,\alpha)=\frac{2\theta}{\alpha-2}\,{}_2F_1\left(1,1-\frac{2}{\alpha};2-\frac{2}{\alpha};-\theta\right). \tag{9}$$

Proof The proof follows from the law of total probability and the fact that sets in (4) are disjoint and can be found in [15]. □

One important point is that (6) is a fixed-point equation of p_k, which approximates the probability of a typical user being a type k user [15, Theorem 1], $\mathcal{P}_N$ is the conditional coverage probability of type N user in the non-full interference network [15, Corollary 1]. Two other corollaries of importance are deduced from Corollary 1.

Corollary 2 *Given* α *and* θ_1*, the probability of being the cell center user* ($k=1$ *in* (6)) *is given as*

$$p_c=p_1=\frac{1}{2}\,{}_2F_1\left(\frac{1}{2},1;2;-4\rho(\theta_1,\alpha)\right). \tag{10}$$

Proof The proof follows from (6) and using $\left(\frac{\sqrt{1+x}-1}{x}\right)^a=2^{-a}\,{}_2F_1\left(\frac{a}{2},\frac{a+1}{2};a+1;-x\right)$. □

Corollary 3 *Given* α *and classification thresholds* $\{\theta_k\}_{1\le k\le N}$*, we have*

$$\mathcal{P}_{\text{cov}}\left(\{\theta_k\}_{k=1}^{N},\alpha,\lambda\right)\le\mathcal{P}_{\text{cov}}\left(\{\theta_k\}_{k=1}^{M},\alpha,\lambda\right),\ \forall N\le M \tag{11}$$

Proof Referring to (4), for $M = N + 1$, we can write

$$\begin{aligned}\mathcal{P}_{\text{cov}}\left(\{\theta_k\}_{k=1}^{N}, \alpha, \lambda\right) &= \mathbb{P}\left(X_0 \in \Phi_1 \cup \cdots \cup \Phi_{N-1} \cup \left\{\Phi_N, \text{SIR}_0^N \geq \theta_N\right\}\right) \\ &\leq \mathbb{P}\left(X_0 \in \Phi_1 \cup \cdots \cup \Phi_{N-1} \cup \left\{\underbrace{\Phi_N, \text{SIR}_0^N \geq \theta_N}_{\Phi_N' \subseteq \Phi_N}\right\} \cup \right. \\ &\quad \left. \left\{\underbrace{\Phi_N, \text{SIR}_0^N < \theta_N}_{\Phi_{N+1} \subseteq \Phi_N}, \text{SIR}_0^{N+1} \geq \theta_{N+1}\right\}\right) \\ &= \mathbb{P}\left(X_0 \in \Phi_1 \cup \cdots \cup \Phi_{N-1} \cup \Phi_N' \cup \left\{\Phi_M, \text{SIR}_0^M \geq \theta_M\right\}\right) \\ &= \mathcal{P}_{\text{cov}}\left(\{\theta_k\}_{k=1}^{M}, \alpha, \lambda\right).\end{aligned}$$

□

Corollary 3 ensures that the increase in the number N of user types cannot decrease the coverage probability. It is important to consider SE as well as coverage since the coverage does not take the resource used into consideration. The following is a description of how the proposed classification impacts SE.

3.2 Spectral efficiency

Considering the system setting of [31], where only one type of user is considered with full interference, the average SE per RB for the typical user is $\mathbb{E}[\ln(1 + \text{SIR})]$. In our case, a given RB is divided into N subchannels, each assigned to its corresponding user type. Each type k user transmits over the kth subchannel. Then, the achievable SE of the typical type k user on the subchannel k is defined as

$$\mathcal{R}_k \triangleq \mathbb{E}\left[\ln\left(1 + \text{SIR}_0^k\right) | X_0 \in \Phi_k\right] \tag{12}$$

where the expectation is taken over the network geometry and channel gains. Then, the weighted SE in nats/s/Hz of the typical user of type k can be written as

$$\eta_k(\omega_k) = \omega_k \mathcal{R}_k, \tag{13}$$

where $0 \leq \omega_k \leq 1$ is the fraction of the given RB according to subchannel k, with $\sum_{k=1}^{N} \omega_k = 1$. The term $\mathcal{R}_k, \forall k \in [\![1, N]\!]$, has been obtained in [15, Theorem 2] as

$$\mathcal{R}_k = \frac{1}{p_k}\left(p_k \ln(1 + \theta_k) + \int_{\theta_k}^{\infty} g_k(z)\mathrm{d}z\right), \tag{14}$$

where

$$g_k(z) = \frac{1}{1+z}\int_0^{\infty} e^{-\nu(1+p_k\rho(z,\alpha))} \prod_{i=1}^{k-1}\left(1 - e^{-p_i\rho(\theta_i,\alpha)\nu}\right)\mathrm{d}\nu, \tag{15}$$

and

$$\mathcal{R}_N = \int_0^\infty \int_0^\infty \frac{e^{-\nu(1+p_N\rho(e^u-1,\alpha))}}{p_N} \prod_{i=1}^{N-1} \left(1 - e^{-p_i\rho(\theta_i,\alpha)\nu}\right) \mathrm{d}\nu \mathrm{d}u. \tag{16}$$

Hence, the average SE $\overline{\eta}$ of the typical user in the non-full interference network is $\overline{\eta} = \sum_{k=1}^{N} p_k \eta_k$.

4 Coverage and spectral efficiency with cooperation

In this section, we investigate a BS cooperation scheme [32] to improve the performance of the typical type N user. Precisely, our proposed scheme exploits the fact that a BS that serves a type k user in another cell is only active on the kth subchannel and remains idle for all the other subchannels and in particular for the Nth subchannel, i.e., the one used by the cell edge user.

4.1 *N* type user classification

Recalling Fig. 1 and the fact that a type N user's cooperation set consists in the $N-1$ closest BS of class $k \in [\![1, N-1]\!]$ plus its BS on subchannel N, the tagged type N user selects the BS among the cooperation set with the best channel quality, while the remaining $N-1$ BS stay silent in the Nth subchannel. Here, the channel quality is the product of the large-scale path loss and the small-scale fading. The user has the opportunity to change its firstly associated BS, based on distance, to another BS with a better channel quality. Let $\mathcal{C}_o = \left\{X^k \triangleq \arg\min_{X_i} \|X_i\| : X_i \in \Phi_k,\ 1 \le k \le N-1\right\}$ be the set of BS that are the nearest type k BS to the typical type N user. Hence, the SIR of the typical type N user is $\mathrm{SIR}_0^N = \frac{S_N}{I_N}$, where $I_N = \sum_{k=1}^{N} I_{N,k}$, and

$$S_N = \max_{X_i \in \mathcal{C}_0 \cup X_0} \left\{H_i^N R_i^{-\alpha}\right\}, \tag{17}$$

$$I_{N,k} = \sum_{X_i \in \Phi_k \setminus \mathcal{C}_0} H_i^N R_i^{-\alpha} \mathbf{1}_{\mathcal{A}_i^k},\ \forall\, 1 \le k \le N \tag{18}$$

with

$$\mathbf{1}_{\mathcal{A}_i^k} = \begin{cases} 1 & \text{if the type-}k\text{ BS } X_i \text{ is selected to serve a type-}N\text{ user} \\ 0 & \text{otherwise} \end{cases}. \tag{19}$$

The main intermediate stage in analyzing the proposed OPS's efficiency is to characterize the joint distribution of the distance between the typical user and the set of candidate BS to cooperate. Let $T_k = \min_{X_i \in \Phi_k} R_i$, for $1 \le k \le N-1$, be the distance of the typical type N user to the nearest BS serving a type k user. Moreover, let G_k, for $1 \le k \le N-1$, be the fading gain between the typical type N user and its nearest type k BS on the Nth subchannel of the RB.

4.1.1 Joint distances distribution

The following lemma gives the joint probability density function (PDF) of $\boldsymbol{T} = [T_1, \ldots, T_{N-1}, R_0]$.

Lemma 1 *Conditioning on the distance of a typical type N user from its nearest BS R_0, the PDF of the distance between the typical user and the nearest helping BS which serves a type k user $T_k, 1 \leq k \leq N-1$, is*

$$f_{T_k|R_0}(t_k \mid r_0, t_k > r_0) = 2\pi\lambda p_k t_k \exp\left(-\pi\lambda p_k\left(t_k^2 - r_0^2\right)\right). \tag{20}$$

Proof The void probability of a 2-D Poisson process Φ_k with density $\lambda_k = p_k\lambda$ in an area A is $\exp(-\lambda_k A)$. The cumulative distribution function of the distance T_k from the typical user to the nearest BS in Φ_k conditioning on $T_k > R_0$ is

$$F_{T_k|R_0}(t_k \mid r_0, t_k > r_0) = 1 - \exp\left(-\pi\lambda_k\left(t_k^2 - r_0^2\right)\right). \tag{21}$$

By taking the derivative of (21) with respect to t_k and knowing that in our model $\lambda_k = p_k\lambda$, we can derive (20). □

Using Lemma 1 and knowing that different types of BS come from disjoint sets, the joint conditional PDF of $\boldsymbol{T}$ given R_0 is $\prod_{k=1}^{N-1} f_{T_k|R_0}(t_k \mid r_0, t_k > r_0)$. Then, unconditioning it by the PDF of R_0, i.e., $f_{R_0}(r_0) = 2\pi\lambda r_0 e^{-\pi\lambda r_0^2}$, gives the joint distances distribution on $\left\{T_k > R_0, k \in [\![1, N-1]\!]\right\}$ as

$$f_{\boldsymbol{T}}(t_1, \ldots, r_0) = (2\pi\lambda)^N r_0\left(\prod_{k=1}^{N-1} p_k t_k\right)\exp\left(-\pi\lambda\sum_{k=1}^{N-1} p_k t_k^2\right)\exp\left(-\pi\lambda\left(1 - \sum_{k=1}^{N-1} p_k\right)r_0^2\right). \tag{22}$$

4.1.2 Laplace transform of the interference

According to (18), the Laplace transform of the interference is given by

$$\mathcal{L}_{I_N}(s) = \mathbb{E}_{I_{N,k}}\left[\exp\left(-s\sum_{k=1}^{N} I_{N,k}\right)\right] = \prod_{k=1}^{N}\mathcal{L}_{I_{N,k}}(s), \tag{23}$$

where

$$\begin{aligned}\mathcal{L}_{I_{N,k}}(s) &= \mathbb{E}\left[\exp\left(-s\sum_{X_i\in\Phi_k\setminus\mathcal{C}_0} H_i^N R_i^{-\alpha}\mathbf{1}_{\mathcal{A}_i^k}\right)\right] \\ &\overset{(a)}{=} \mathbb{E}_{\Phi,\{H_i^N\}}\left[\prod_{X_i\in\Phi_k\setminus\mathcal{C}_0}\left(\mathbb{E}[\mathbf{1}_{\mathcal{A}_i^k}]e^{-sH_i^N R_i^{-\alpha}} + (1 - \mathbb{E}[\mathbf{1}_{\mathcal{A}_i^k}])\right)\right] \\ &\overset{(b)}{=} \mathbb{E}_{\Phi}\left[\prod_{X_i\in\Phi_k\setminus\mathcal{C}_0} 1 - \mathbb{E}[\mathbf{1}_{\mathcal{A}_i^k}]\left(1 - \frac{1}{1 + sR_i^{-\alpha}}\right)\right]\end{aligned} \tag{24}$$

where (a) follows the law of total expectation, i.e., $\mathbb{E}_X[f(X)] = \mathbb{E}_Y[\mathbb{E}_X[f(X)|Y]]$, (b) comes from averaging over the i.i.d. exponential distribution of interfering fading channels H_i^N with mean 1, as in [31], and factoring out the term $\mathbb{E}[\mathbf{1}_{\mathcal{A}_i^k}]$. Finally by applying the probability generating function (PGFL) of a PPP [33], we have

$$\mathcal{L}_{I_{N,k}}(s) = \exp\left(-2\pi\lambda_k p_{a_k}\int_{t_k}^{\infty}\frac{sr}{r^\alpha + s}\mathrm{d}r\right) = \exp\left(-\pi\lambda p_k p_{a_k}\rho(st_k^{-\alpha},\alpha)t_k^2\right), \quad (25)$$

where p_{a_k} is the probability that a BS serving a type k user is selected by OPS to help the typical type N user. Hence,

$$p_{a_k} = \mathbb{P}\left(G_1 T_1^{-\alpha} < G_k T_k^{-\alpha}, \cdots, H_0^N R_0^{-\alpha} < G_k T_k^{-\alpha}\right), \forall k \in [\![1, N-1]\!]. \quad (26)$$

Similarly, for $k = N$,

$$\mathcal{L}_{I_{N,N}}(s) = \exp\left(-\pi\lambda\left(1 - \sum_{k=1}^{N-1} p_k\right)p_{a_N}\rho(sr_0^{-\alpha},\alpha)r_0^2\right). \quad (27)$$

Remark Based on the cooperation set definition, it is possible to have the same BS in the cooperation set of different type N users in the model. Moreover, in Sect. 2, we consider that each BS could serve only one user in the relative subchannel of the RB. Hence, if OPS scheme selects the same type k BS for two or more type N users, the selected BS can only serve one type N user, and other type N users must search for another BS in their cooperation set.

According to the above remark, quantifying the probability that one cooperative BS be selected by two or more type N users is a complex problem. However, the density of type N users can be relatively lower than other type of users based on the number of user classes and the classification threshold $\{\theta_k\}_{k=1}^{N-1}$ (see Fig. 1). Therefore, it is assumed that the common cooperative BS in the cooperation sets of different type N users can be neglected. The numerical results will show that this assumption is reasonable and leads to tight approximation.

The probability that OPS technique selects the first associated type N BS is p_{a_N}, used in (27), and it is the complementary event of all cooperation events in (26). Hence, we can write

$$p_{a_N} = 1 - \sum_{k=1}^{N-1} p_{a_k}. \quad (28)$$

The probabilities p_{a_k} are given by the following theorem.

Theorem 1 *Given that OPS is applied to the cooperation set of a typical type N user, the probability that a type k BS is selected to serve the typical type N user is*

$$p_{a_k} = \int_0^\infty \int_0^\infty \int_{B^c(0,r_0)^{N-1}} e^{-g}\left(1-e^{-\left(\frac{r_0}{t_k}\right)^\alpha g}\right)\prod_{\substack{m=1\\m\neq k}}^{N-1}\left(1-e^{-\left(\frac{t_m}{t_k}\right)^\alpha g}\right) \times f_{T_1,\cdots,T_{N-1},R_0}(t_1,\cdots,t_{N-1},r_0)\,\mathrm{d}t_1\cdots\mathrm{d}t_{N-1}\mathrm{d}r_0\mathrm{d}g, \tag{29}$$

where $B^c(0,r_0)$ denotes the complement of $B(0,r_0)$, which is a ball centered at the origin with radius r_0.

Proof Referring to (26) and knowing that $\{\{G_m\}_{m=1}^{N-1}, H_0^N\}$ are i.i.e.d., by conditioning on G_k and on the distances distribution $\boldsymbol{T}$, we can write

$$\begin{aligned} p_{a_k} &= \mathbb{E}_{\boldsymbol{T}}\mathbb{E}_{G_k}\left[\mathbb{E}_{G_1}\left[\mathbf{1}\left(G_1 < G_k\left(\frac{T_1}{T_k}\right)^\alpha\right)\right]\times\cdots\times\mathbb{E}_{H_0^N}\left[\mathbf{1}\left(H_0^N < G_k\left(\frac{R_0}{T_k}\right)^\alpha\right)\right]\right] \\ &= \mathbb{E}_{\boldsymbol{T}}\mathbb{E}_{G_k}\left[\prod_{\substack{m=1\\m\neq k}}^{N-1}\mathbb{E}_{G_m}\left[\mathbf{1}\left(G_m < G_k\left(\frac{T_m}{T_k}\right)^\alpha\right)\right]\times\mathbb{E}_{H_0^N}\left[\mathbf{1}\left(H_0^N < G_k\left(\frac{R_0}{T_k}\right)^\alpha\right)\right]\right] \\ &= \mathbb{E}_{\boldsymbol{T}}\mathbb{E}_{G_k}\left[\prod_{\substack{m=1\\m\neq k}}^{N-1}\left(1-\exp\left(-\left(\frac{T_m}{T_k}\right)^\alpha G_k\right)\right)\times\left(1-\exp\left(-\left(\frac{R_0}{T_k}\right)^\alpha G_k\right)\right)\right]. \end{aligned} \tag{30}$$

The proof ends by averaging over G_k and $\boldsymbol{T}$. □

4.1.3 Type N user coverage probability

We derive the coverage probability of the typical type N user using the joint distribution of distances from its cooperation set BS, given in (22).

Theorem 2 *Given that OPS is applied to the cooperation set of a typical type N user, the coverage probability of the typical type N user is given by*

$$\begin{aligned} \mathcal{P}_N\left(\{\theta_k\}_{k=1}^N,\alpha,\lambda\right) = 1 - \frac{1}{p_N}\int_0^\infty\int_{B^c(0,r_0)^{N-1}}&\left(1-\mathcal{L}_{I_N}(\theta_N r_0^\alpha)\right) \\ &\times\prod_{k=1}^{N-1}\left(1-\mathcal{L}_{I_N}(\theta_N t_k^\alpha)\right)\left(1-\mathcal{L}_{I_{0,k}}(\theta_k r_0^\alpha)\right) \\ &\times f_{T_1,\cdots,T_{N-1}R_0}(t_1,\cdots,t_{N-1},r_0)\mathrm{d}t_1\cdots\mathrm{d}t_{N-1}\mathrm{d}r_0. \end{aligned} \tag{31}$$

where $\mathcal{L}_{I_N}(s)$ is obtained by (23) and

$$\mathcal{L}_{I_{0,k}}(s) = \exp\left(-\pi\lambda p_k \rho(s r_0^{-\alpha},\alpha) r_0^2\right). \tag{32}$$

Proof See Appendix 8.1. □

4.1.4 Type N user spectral efficiency

Similar to [15, Theorem 2], SE of the typical type N user under OPS scheme can be written as

$$\mathcal{R}_N = \int_0^\infty \mathcal{P}_N\left(\{\theta_k\}_{k=1}^{N-1}, \theta_N = e^u - 1, \alpha, \lambda\right) \mathrm{d}u. \tag{33}$$

4.2 Two user types classification

As a particular case, let us consider the non-full interference network with two user types in the network. In this case, type 1 and type 2, called cell center and cell edge users, are present in the network. The given RB is divided into cell center and cell edge subchannels. In the following, the closed-form expressions for the conditional coverage probability and the spectral efficiency of the typical cell edge user under OPS scheme are derived.

4.2.1 Cooperation probability

The probability that a BS serving a cell center user be selected by OPS to cooperate in the second (cell edge) subchannel of the scheduled resource is

$$p_a = \mathbb{P}\left(G_1 T_1^{-\alpha} > H_0^2 R_0^{-\alpha}\right), \tag{34}$$

where G_1 is the cooperation gain in the second subchannel, H_0^2 is the gain between the tagged BS and its cell edge user, T_1 is the distance between the typical cell edge user and the nearest cooperative BS, and R_0 is the distance between the tagged BS and the cell-edge user. The probability p_a can be computed with the following lemma.

Lemma 2 *The probability that a typical BS serving a cell center user be called for a cooperation is*

$$p_a = 1 - \sum_{k=0}^{\infty} \frac{2\, p_c (-1)^k}{\alpha k + 2}\, {}_2F_1\left(2, 1; \frac{\alpha k}{2} + 2; 1 - p_c\right). \tag{35}$$

Proof See Appendix 8.2. □

4.2.2 Type 2 user coverage probability

The coverage probability of a typical cell edge user when OPS is applied can be formalized as follows.

Theorem 3 *Given two coverage thresholds θ_1 and θ_2, the coverage probability of a typical cell edge user when OPS is applied in the non-full interference network can be calculated as*

$$\mathcal{P}_2(\theta_1,\theta_2,\alpha)=\frac{1}{1-p_c}\sum_{i=1}^{3}(\mathcal{M}_i(\theta_1,\theta_2,\alpha)-\mathcal{Q}_i(\theta_1,\theta_2,\alpha)), \tag{36}$$

where $\mathcal{M}_i$ *and* $\mathcal{Q}_i$, $i\in\{1,2,3\}$, *are*

$$\begin{aligned}
\mathcal{M}_1&=\int_0^1\frac{p_c\mathrm{d}x}{\mathcal{K}^2\left(x,\rho(\theta_2x^{\frac{\alpha}{2}},\alpha),\rho(\theta_2,\alpha)\right)},\\
\mathcal{M}_2&=\int_0^1\frac{p_c\mathrm{d}x}{\mathcal{K}^2\left(x,\rho(\theta_2,\alpha),\rho(\theta_2x^{-\frac{\alpha}{2}},\alpha)\right)},\\
\mathcal{M}_3&=\int_0^1\frac{-p_c\mathrm{d}x}{\mathcal{K}^2\left(x,\rho(\theta_2,\alpha)+\rho(\theta_2x^{\frac{\alpha}{2}},\alpha),\rho(\theta_2,\alpha)+\rho(\theta_2x^{-\frac{\alpha}{2}},\alpha)\right)},\\
\mathcal{Q}_1&=\int_0^1\frac{p_c\mathrm{d}x}{\left(p_c\,\rho(\theta_1,\alpha)x+\mathcal{K}(x,\rho(\theta_2x^{\frac{\alpha}{2}},\alpha),\rho(\theta_2,\alpha))\right)^2},\\
\mathcal{Q}_2&=\int_0^1\frac{p_c\mathrm{d}x}{\left(p_c\,\rho(\theta_1,\alpha)x+\mathcal{K}(x,\rho(\theta_2,\alpha),\rho(\theta_2x^{-\frac{\alpha}{2}},\alpha))\right)^2},\\
\mathcal{Q}_3&=\int_0^1\frac{-p_c\mathrm{d}x}{\left(p_c\,\rho(\theta_1,\alpha)x+\mathcal{K}\left(x,\rho(\theta_2,\alpha)+\rho(\theta_2x^{\frac{\alpha}{2}},\alpha),\rho(\theta_2,\alpha)+\rho(\theta_2x^{-\frac{\alpha}{2}},\alpha)\right)\right)^2},\\
\mathcal{K}(x,\kappa_1,\kappa_2)&=p_c+(1-p_c)p_a\kappa_1+(1-p_c)(1+(1-p_a)\kappa_2)x.
\end{aligned} \tag{37}$$

Proof See Appendix 8.3. □

In the next section, the performance of widely studied bandwidth allocation strategies is investigated under the theoretical non-full interference framework developed in this paper. In particular, the trade-off between SE and fairness of the identified strategies is investigated.

5 Bandwidth allocation

From (13), the network's spectral efficiency $\boldsymbol{\eta}=[\eta_1,...,\eta_N]$ is a function of individual BWP $\boldsymbol{\omega}=[\omega_1,...,\omega_N]$. Hence, the bandwidth allocation strategy plays an important role in the performance achieved.

5.1 Max-mean BWP strategy

The first BWP strategy tries to maximize the mean SE and is expressed as

$$\begin{aligned}
\mathscr{P}_1:\quad &\max_{\boldsymbol{\omega}}\quad \sum_k p_k\eta_k(\omega_k)\\
\text{s.t.}\quad &C_1:\quad \omega_k\geq 0,\quad \forall\, k\in[\![1,N]\!]\\
&C_2:\quad \sum_k\omega_k=1,\\
&C_3:\quad \sum_k p_k=1.
\end{aligned} \tag{38}$$

The optimal solution is simply given by $\omega_k=1$ for the index k corresponding to the largest value of $\mathcal{R}_k$, which is a function of the set of classification thresholds, and $\omega_k=0$ otherwise [15]. However, this allocation does not take into account fairness among

different users; it only aims at maximizing the sum of SE of all users. It can be preferable to share the RB among all the covered users, i.e., $\omega_k > 0$ for all k.

5.2 Uniform BWP strategy

The simplest partition policy, which does not need any other information from the system, is the equal partitioning method where the RB is equally divided into N subchannels, i.e., $\omega_k = 1/N, \forall k$. In this case, the weighted SE of the typical user is [15 Subsection III-C]

$$\overline{\eta} = \frac{1}{N}\left(\sum_{k=1}^{N-1}\left(p_k \ln(1+\theta_k) + \int_{\theta_k}^{\infty} g_k(z)\mathrm{d}z\right) + p_N \mathcal{R}_N\right). \tag{39}$$

5.3 SIR-proportional BWP strategy

The third strategy is the adaptive bandwidth partition, where the available bandwidth is shared among the users according to the SIR distribution and traffic load [10]. Hence, in the SIR-proportional model, we have $\omega_k = p_k$, and the mean SE is [15 Subsection III-C]

$$\overline{\eta} = \sum_{k=1}^{N-1}\left(p_k^2 \ln(1+\theta_k) + p_k \int_{\theta_k}^{\infty} g_k(z)\mathrm{d}z\right) + p_N^2 \mathcal{R}_N. \tag{40}$$

5.4 Max-min BWP strategy

The fourth used strategy is named max-min criterion proposed in [34]. It aims at gaining the worst-case performance by maximizing the lowest rate among all user types as

$$\begin{array}{lll} \mathscr{P}_2: & \max\limits_{\boldsymbol{\omega}} \min\limits_{\eta_k} & \eta_k(\omega_k) \\ \text{s.t.} & C_1, C_2, C_3. & \end{array} \tag{41}$$

The solution is achieved when all SE are equal, i.e., $\eta_i = \eta_j, \forall i, j \in [\![1, N]\!]$. Hence, the partition ω_k allocated to the kth user is directly given by

$$\omega_k = \frac{1}{\mathcal{R}_k}\left(\sum_k \frac{1}{\mathcal{R}_k}\right)^{-1}. \tag{42}$$

The max-min criterion gives a kind of fairness since each user has the same spectral efficiency, but in the same time, this strategy leads to a poor global sum-rate. The trade-off between the fairness and the maximum sum-rate in the network can be seen as an attempt to control the variance of the SE allocated to users in the network [35, 36]. In the following, we study a mean–variance trade-off-based BWP with a given value of the trade-off level.

5.5 Mean–variance trade-off-based BWP strategy

In this section, instead of maximizing the average SE, we introduce the concept of risk to ensure maximum network SE subject to a certain level of fairness among all user types

in the network. In particular, we use the expected exponential utility risk model [28, 35], which is defined as follows:

$$\begin{aligned}\mathcal{H}(\boldsymbol{\omega}) &= \frac{1}{\beta}\log\left[\mathbb{E}[\exp(\beta\boldsymbol{\eta})]\right] \\ &= \frac{1}{\beta}\log\left[\sum_k p_k\, e^{\beta\eta_k(\omega_k)}\right].\end{aligned} \tag{43}$$

where β is an appropriately chosen constant known as the risk sensitivity parameter. The above function is the aversion for the risk when $\beta < 0$ and risk-seeking if $\beta > 0$. Expanding the Maclaurin series of the log and exp functions indicates that (43) catches higher-order moments of BWP. Concretely, in small risks, the exponential utility function is provided as [35]:

$$\mathcal{H}(\boldsymbol{\omega}) = \mathbb{E}[\boldsymbol{\eta}] + \frac{\beta}{2}\,\mathrm{Var}[\boldsymbol{\eta}] + \mathcal{O}(\beta^2). \tag{44}$$

where $\mathbb{E}[\boldsymbol{\eta}] \triangleq \sum_{k=1}^{N} p_k\eta_k$, $\mathrm{Var}[\boldsymbol{\eta}] \triangleq \sum_{k=1}^{N} p_k(\eta_k - \mathbb{E}[\boldsymbol{\eta}])^2$. The variance term controls the variability of the SE among user types and can be used to control the fairness among users. Therefore, the bandwidth partitioning problem based on a given level of fairness can be formulated as the following optimization problem:

$$\begin{aligned}\mathscr{P}_4: \quad &\max_{\boldsymbol{\omega}} \quad \tfrac{1}{\beta}\log\left[\textstyle\sum_k p_k\, e^{\beta\eta_k(\omega_k)}\right] \\ \text{s.t.} \quad &C_1, C_2, C_3.\end{aligned} \tag{45}$$

The objective function in (45) has a positive Hessian w.r.t. $\boldsymbol{\omega}$ for $\beta > 0$ and a negative Hessian for $\beta < 0$. Hence, in the risk-averse setting, the utility function is concave w.r.t. $\boldsymbol{\omega}$. Moreover, the feasible region has the convexity property since the constraints C_1 and C_2 are linear constraints. Therefore, for a given $\{\theta_k\}_{1\le k\le N}$ and α, (45) is a convex optimization problem.

The optimization problem formulated in (45) is a standard nonlinear programming problem that can be solved using the Karush–Kuhn–Tucker (KKT) conditions [37]. The Lagrangian function expresses as follows:

$$L(\boldsymbol{\omega}, \mu, \boldsymbol{\xi}) = \frac{1}{\beta}\log\left[\sum_k p_k\, e^{\beta\eta_k(\omega_k)}\right] + \mu(1 - \sum_k \omega_k) + \sum_k \xi_k\omega_k, \tag{46}$$

where μ and ξ_k are the KKT multipliers. Subsequently, the KKT conditions give

$$\begin{cases} \frac{\partial L}{\partial \omega_i} = \frac{p_i\mathcal{R}_i\exp(\beta\eta_i(\omega_i))}{\sum_k p_k\,\exp(\beta\eta_k(\omega_k))} - \mu + \xi_i = 0, \quad \forall\, i \in [\![1, N]\!] \\ 1 - \sum\limits_k \omega_k = 0 \\ \xi_k\omega_k = 0, \quad \forall\, k \in [\![1, N]\!] \\ \sum\limits_k p_k = 1. \end{cases} \tag{47}$$

Solving the system of equations in (47) yields the optimal BWP with adequate fairness. The system can be solved using the water-filling algorithm proposed in [38]. From the above results, we can write the water-filling value ω_i as a function of the Lagrange multiplier μ, i.e., $\omega_i = f_i(\mu)$, where

$$f_i(\mu) = \frac{1}{\beta \mathcal{R}_i} \log \left[\frac{\mu \sum_{k \in [\![1,N]\!] \setminus \{i\}} p_k \exp(\beta \eta_k(\omega_k))}{p_i \cdot (\mathcal{R}_i - \mu)} \right]. \tag{48}$$

Considering that ω_i must be nonnegative (C_1), the water-filling value can be represented as follows:

$$\omega_i = \begin{cases} f_i(\mu) & \text{if } f_i(\mu) > 0 \\ 0 & \text{otherwise} \end{cases}. \tag{49}$$

Finally, the Lagrange multiplier μ is obtained using the primal feasibility (C_2) as

$$\sum_i f_i(\mu) \mathbf{1}(f_i(\mu) > 0) = 1. \tag{50}$$

From (50), no closed-form expression for ω_i as a function of μ independent from $\{\omega_k, \forall\, k \in [\![1,N]\!] \setminus \{i\}\}$ can be obtained. However, for a given network realization, the solution can be iteratively estimated via a bisection search algorithm like in [38]. Bisection search is a simple method with very high performance. However, the starting points of the algorithm have to be chosen carefully. The following corollary bounds the possible value of the Lagrangian multiplier μ.

Corollary 4 *Given p_k and η_k for all $k \in [\![1,N]\!]$, the water-filling value μ should satisfy*:

$$\underbrace{0}_{\mu_{\min}} \leq \mu \leq \underbrace{\min_i \left(\frac{p_i \mathcal{R}_i}{p_i + \sum_{k \in [\![1,N]\!] \setminus \{i\}} p_k \exp(\beta \eta_k(\omega_k))} \right)}_{\mu_{\max}}. \tag{51}$$

Proof The proof follows from (49) and the fact that β takes a negative value in the risk-averse model, which limits the argument of the logarithm function to be positive and less than 1. □

Each of the BWP strategies addressed in this section has its own merit in fairness. To compare the fairness gain of the different BWP strategies, we use the Jain's index, since it is a widely used metric in literature [39, 40]. The definition of Jain's index is formulated as follows.

Definition 1 Given a set of achievable SE $\eta_k : k = 1, ..., N$, the corresponding Jain's index is

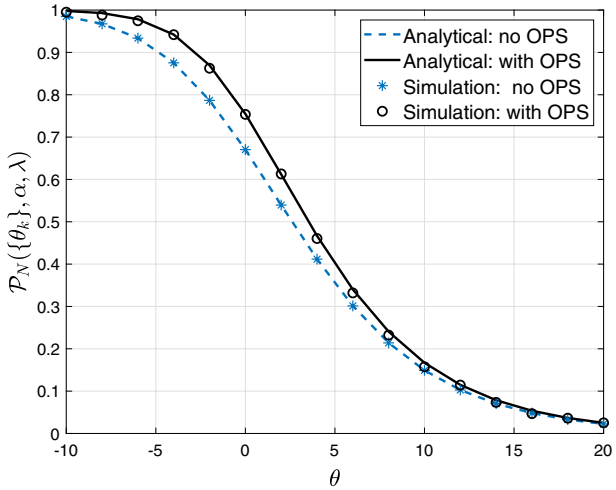

Fig. 2 Cell edge user coverage probability using OPS with $N = 2$ partitions

$$\mathcal{F}(\boldsymbol{\omega}) = \frac{\left[\sum_k p_k \eta_k(\omega_k)\right]^2}{\sum_k p_k \eta_k^2(\omega_k)}. \tag{52}$$

where $\mathcal{F}(\boldsymbol{\omega})$ gives a continuous value in the range of $\left[\min_k\{p_k\}, 1\right]$.

6 Results and discussion

Simulations are conducted in a PPP network. The coverage probability and SE are evaluated at the typical user for 100,000 network realizations. The standard power-law path loss model with exponent $\alpha > 2$ is considered for signal propagation. We assume that all BS and users are equipped with a single antenna, and users are experiencing an independent block Rayleigh fading channel on each RB. We consider an interference-limited scenario with $\alpha = 4$, i.e., without thermal noise at the receiver. We investigate the average SE per unit RB where a given RB is divided into N sub-channels. At each realization, the BS locations are generated as a PPP of unit intensity in an area of $[-30, 30] \times [-30, 30]$, and user density is considered large enough to have at least one user per cell.

Figure 2 shows the simulation and analytical results of the cell edge coverage probability in the case of two user types (36) with/without OPS in the non-full interference network with a unique classification threshold. From the figure, the coverage probability of the cell edge user is enhanced under OPS compared to the noncooperative scenario. When the unique threshold increases, both techniques converge because the number of BS serving a type 1 user in the network decreases. Moreover, simulation and analytical results match, which validates the theoretical findings of Sect. 4.

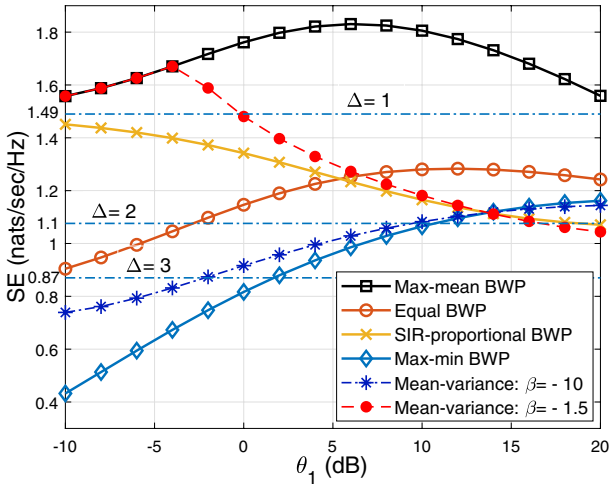

Fig. 3 SE under different BWP strategies $\beta = -1.5\,\beta = -10$.

Figure 3 compares the average SE for the cell center/edge user classification in the non-full interference scenario versus the type 1 user target threshold θ_1 under different BWP strategies. Moreover, the achieved average SE is compared with the conventional frequency reuse technique with reuse factor Δ presented in [31]. The figure depicts that the max-mean BWP outperforms other strategies, since giving all the bandwidth to the best user is optimal regarding the network SE performance. Moreover, the curve corresponding to the max-mean SE first increases and then decreases after almost 8 dB, because for small values of θ_1, almost all users are in the cell center. On the other hand, large values of θ_1 make all users be cell edge users, and it tends to the full interference case, i.e., frequency reuse with $\Delta = 1$. Moreover, it can be clearly observed that when θ_1 increases, the average SE under SIR-proportional policy (40) decreases while SE increases under equal partitioning (39). It can be seen that equal BWP eventually outperforms SIR-proportional BWP by increasing θ_1 above 5 dB. This is because, contrary to equal BWP, SIR-proportional BWP gives more bandwidth to cell edge users when θ_1 increases, that is less efficient for the global SE. Indeed, in SIR-proportional policy, the typical user benefits from a fraction of resources that depends on the SIR and suffers from the same fraction of the interference. However, SIR-proportional policy still has a higher SE than static frequency reuse with $\Delta = 2$. Besides, the figure compares the mean–variance BWP (45) according to the risk sensitivity level β with other BWP policies. For $\beta = -1.5$, the mean–variance BWP is a weak risk-averse policy and attempts to maximize the network SE by giving more bandwidth to the cell center users. Hence, the SE achieved by mean–variance BWP is identical to the max-mean strategy for small θ_1 and then decreases when θ_1 increases. This is because the number of cell center users decreases by increasing the threshold value, and the policy tends to limit the increase in the variance in the rate allocation.

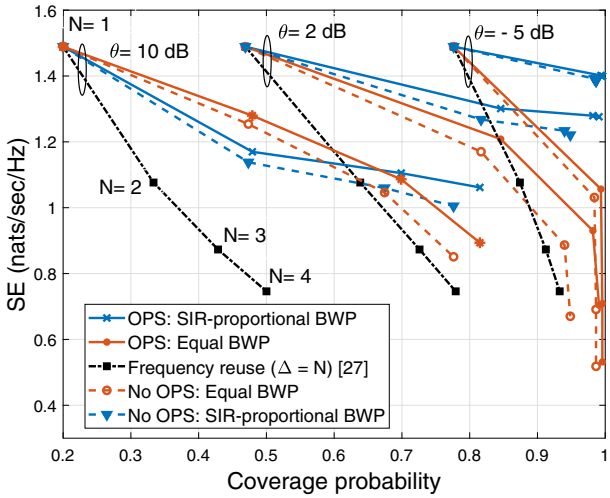

Fig. 4 SE–coverage trade-off for different BWP strategies with several number of user classes

On the other hand, if $\beta = -10$, the policy is even more risk-averse and tends to ensure fairness among users in the Jain's index sense. It also means that by decreasing β, the SE achieved by the mean–variance strategy tends to the one obtained with the max-min BWP (41). Max-min BWP consists in giving the same amount of rate among user types and hence minimizing the variance of the allocation and SE increases by increasing θ.

Figure 4 compares the network average SE–coverage probability trade-off for SIR-proportional BWP, equal BWP and frequency reuse (with $\Delta = N$) with/without BS cooperation technique, i.e., OPS scheme, and for unique threshold value θ ranging in $\{-5, 2, 10\}$ dB. Whatever the BWP scheme considered, the coverage probability increases, whereas the average SE decreases when N increases, but with different trends according to the threshold θ. However, the curves corresponding to the SIR-proportional and equal BWP policies are above the conventional frequency reuse. Furthermore, for $\theta \in \{-5, 2\}$ dB, the average SE achieved with SIR-proportional BWP is higher because it allocates more bandwidth to the type 1 user, which has a higher achievable spectral efficiency than other user types in the network. In contrast, equal BWP equally allocates bandwidth regardless of the density of the different user types in the network. On the other hand, for $\theta = 10$ dB and $N = 2$, equal BWP has a higher SE than SIR-proportional BWP. This is due to the fact that a high threshold value shrinks the cell center region, and the SIR-proportional approach allocates more bandwidth to the cell edge user, which has a lower SE than the cell center user. But, when N increases, SIR-proportional achieves again higher SE than equal BWP. This is because the negative effect of equally dividing the available bandwidth is greater than the density-dependent allocation based on the user type. Finally, OPS strategy improves the trade-off front by increasing the SE

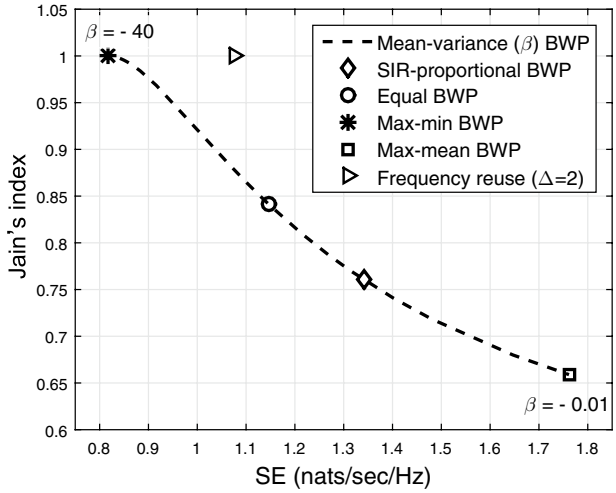

Fig. 5 Fairness–SE trade-off under different BWP strategies for $N = 2$ and $\theta = 0$ dB. $\beta = -0.01 \beta = -40$

of the type N user using a BS selection diversity scheme, in particular for moderate-to-high threshold values.

Figure 5 illustrates the Jain's index–average SE trade-off for different strategies investigated in this work. The mean–variance BWP characterizes the trade-off between the network SE and the fairness among user types, when β value decreases from -0.01 to -40. As the network SE decreases, the fairness measured with the Jain's index increases and this index decreases when SE increases. The max-mean BWP has the maximum SE but with the lowest fairness in bandwidth partitioning. By sacrificing SE, SIR-proportional and equal BWPs achieve higher fairness regarding the max-mean strategy. The max-min BWP offers the fairest bandwidth sharing, in the Jain's index sense, while having the lowest SE. One can remark that the frequency reuse technique allows to achieve a larger network SE than the one obtained with the max-min policy with a Jain's index equal to 1. This is because the allocated bandwidth does not depend on the position of the typical user in the cell so the user-type fairness is one. The fairness measured is among user types, and it does not mean that the fairness among users would be one with the frequency reuse technique since users do not experience the same rate. The mean–variance fairness criterion with a given risk level β allows exploring the feasible operational point based on the desired SE and level of fairness among different user types in the cellular network.

7 Conclusion

This paper has presented a complete characterization of a typical user's downlink coverage probability and spectral efficiency in a non-full interference homogeneous PPP network, i.e., when the statistic of the interference depends on the classification

of the users. To help cell edge users in the network, an optimal point selection cooperation scheme was applied, and semi-closed-form expressions of performance metrics based on the typical user's received SIR level have been derived. Then, to maximize the network average spectral efficiency, different bandwidth allocation schemes among user types have been expressed and evaluated. Finally, using the Jain's index, the fairness of the bandwidth allocation schemes has been quantified. Moreover, portfolio theory has been firstly used in our context to assess the trade-off between SE and fairness. Numerical results demonstrated that the user-centric resource allocation approach outperforms the conventional frequency reuse approach, which is BS-centric. We intend to follow the user-centric frequency reuse in non-Poisson models to consider spatial repulsion among BS deployment in future work.

Appendix

Proof of Theorem 2

By using the Bayes rule and recalling (17) and (18), we get

$$\begin{aligned}\mathcal{P}_N(\{\theta_k\}_{k=1}^N,\alpha,\lambda) &= \frac{\mathbb{P}(S_N \geq \theta_N I_N, X_0 \in \Phi_N)}{\mathbb{P}(X_0 \in \Phi_N)} \\ &= 1 - \frac{\mathbb{P}(S_N < \theta_N I_N, X_0 \in \Phi_N)}{\mathbb{P}(X_0 \in \Phi_N)}.\end{aligned} \tag{53}$$

Next, we expand the term $\Xi = \mathbb{P}(S_N < \theta_N I_N, X_0 \in \Phi_N)$ as

$$\begin{aligned}\Xi &= \mathbb{P}\left(\max_{X_i \in \mathcal{C}_0 \cup X_0} \left\{H_i^N R_i^{-\alpha}\right\} < \theta_N I_N, X_0 \in \Phi_N\right) \\ &= \mathbb{P}\left(G_1 T_1^{-\alpha} < \theta_N I_N, \cdots, H_0^N R_0^{-\alpha} < \theta_N I_N, X_0 \in \Phi_N\right) \\ &= \mathbb{E}_{\boldsymbol{T}}\left[\prod_{k=1}^{N-1} \mathbb{P}\left(G_k T_k^{-\alpha} < \theta_N I_N \mid T_k\right) \mathbb{P}\left(H_0^N R_0^{-\alpha} < \theta_N I_N \mid R_0\right) \mathbb{P}(X_0 \in \Phi_N \mid R_0)\right],\end{aligned} \tag{54}$$

where

$$\mathbb{P}(G_k T_k^{-\alpha} < \theta_N I_N \mid T_k) = 1 - \mathcal{L}_{I_N}(\theta_N T_k^{\alpha}), \tag{55}$$

$$\mathbb{P}(X_0 \in \Phi_N \mid R_0) = \prod_{k=1}^{N-1} 1 - \mathcal{L}_{I_{0,k}}(\theta_k R_0^{\alpha}). \tag{56}$$

Proof of Lemma 2

Using the definition of p_a in (34) and by conditioning on the joint distance distribution of T_1 and R_0

$$
\begin{aligned}
p_a &= 1 - \mathbb{E}_{T_1,R_0}\mathbb{E}_{G_1}\left[\mathbb{P}\left(H_0^2 > G_1\left(\frac{R_0}{T_1}\right)^{\alpha}\right)\right] \\
&= 1 - \mathbb{E}_{T_1,R_0}\left[\frac{1}{1+\left(\frac{R_0}{T_1}\right)^{\alpha}}\right] \\
&\overset{(a)}{=} 1 - \sum_{k=0}^{\infty}(-1)^k \mathbb{E}_{T_1,R_0}\left[\left(\frac{R_0}{T_1}\right)^{\alpha k}\right],
\end{aligned}
$$

where (a) comes from $(1+x)^{-1} = \sum_{k=0}^{\infty}(-1)^k x^k$. From the joint distances distribution in (22), the joint PDF of T_1 and R_0 is

$$
f_{T_1,R_0}(t_1, r_0) = p_c(2\pi\lambda)^2 t_1 r_0 e^{-p_c\lambda\pi t_1^2} e^{-(1-p_c)\lambda\pi r_0^2}, \tag{57}
$$

where $r_0 \in [0,\infty)$ and $t_1 \in [r_0,\infty)$. Hence, we have

$$
\begin{aligned}
\mathbb{E}_{T_1,R_0}\left[\left(\frac{R_0}{T_1}\right)^{\alpha k}\right] &= p_c(2\pi\lambda)^2 \int_0^{\infty}\int_{r_0}^{\infty}\left(\frac{r_0}{t_1}\right)^{\alpha k} t_1 r_0 e^{-\lambda\pi\left(p_c t_1^2 + (1-p_c) r_0^2\right)} \mathrm{d}t_1 \mathrm{d}r_0 \\
&\overset{(a)}{=} p_c(2\pi\lambda)^2 \int_0^{\infty}\int_0^{1} u^{\alpha k-3} v^3 e^{-\lambda\pi\left(p_c u^{-2} + (1-p_c)\right)v^2} \mathrm{d}u \mathrm{d}v \\
&\overset{(b)}{=} p_c(2\pi\lambda)^2 \int_0^{1} u^{\alpha k-3} \int_0^{\infty} \frac{y e^{-y} \mathrm{d}y}{2(\pi\lambda)^2\left(p_c u^{-2} + (1-p_c)\right)^2} \mathrm{d}u \\
&= 2p_c \int_0^{1} \frac{u^{\alpha k-3}}{\left(p_c u^{-2} + (1-p_c)\right)^2} \mathrm{d}u \\
&= \frac{p_c^{-1}}{(\frac{\alpha k}{2}+1)} {}_2F_1\left(2, \frac{\alpha k}{2}+1; \frac{\alpha k}{2}+2; \frac{p_c-1}{p_c}\right),
\end{aligned} \tag{58}
$$

where (a) comes from change of variables $\frac{r_0}{t_1} = u$ and $v = r_0$, (b) comes by letting $\lambda\pi\left(1 - p_c\left(1 - \frac{1}{u^2}\right)\right)v^2 = y$. Finally, by applying

$$
{}_2F_1(a,b;c;z) = (1-z)^{-a} {}_2F_1\left(a, c-b; c; \frac{z}{z-1}\right), \tag{59}
$$

and substituting (58) in (57), we can derive (35).

Proof of Theorem 3

Applying Theorem 2 for $N = 2$ leads to

$$
\begin{aligned}
\mathcal{P}_2(\theta_1,\theta_2,\alpha,\lambda) &= 1 - \frac{1}{1-p_c}\int_0^{\infty}\int_{r_0}^{\infty}\left(1 - \mathcal{L}_{I_2}(\theta_2 r_0^{\alpha})\right)\left(1 - \mathcal{L}_{I_2}(\theta_2 t_1)\right) \\
&\quad \times \left(1 - \mathcal{L}_{I_{0,1}}(\theta_1 r_0^{\alpha})\right) f_{T_1,R_0}(t_1, r_0)\, \mathrm{d}t_1 \mathrm{d}r_0 \\
&= \frac{1}{1-p_c}\sum_{i=1}^{3}\left(\mathcal{M}_i(\theta_1,\theta_2,\alpha) - \mathcal{Q}_i(\theta_1,\theta_2,\alpha)\right).
\end{aligned} \tag{60}
$$

We can derive $\mathcal{M}_1$ as follows:

$$\mathcal{M}_1 = \int_0^\infty \int_{r_0}^\infty \mathcal{L}_{I_2}(\theta_2 r_0^\alpha) f_{T_1,R_0}(t_1, r_0)\, \mathrm{d}t_1 \mathrm{d}r_0, \tag{61}$$

where by substituting $\mathcal{L}_{I_2}(\theta_2 r_0^\alpha)$ from (23) into (61), we have

$$\begin{aligned}
\mathcal{M}_1 &= p_c(2\pi\lambda)^2 \int_0^\infty \int_{r_0}^\infty e^{-\lambda\pi p_c p_a \rho(\theta_2(\frac{r_0}{t_1})^\alpha,\alpha)t_1^2} e^{-\lambda\pi(1-p_c)(1-p_a)\rho(\theta_2,\alpha)r_0^2} \\
&\quad \times e^{-\lambda\pi p_c t_1^2} e^{-\lambda\pi(1-p_c)r_0^2} t_1 r_0 \mathrm{d}t_1 \mathrm{d}r_0 \\
&= p_c(2\pi\lambda)^2 \int_0^\infty \int_0^1 e^{-\lambda\pi p_c(1+p_a\rho(\theta_2 u^\alpha,\alpha))u^{-2} r_0^2} e^{-\lambda\pi(1-p_c)(1+(1-p_a)\rho(\theta_2,\alpha))r_0^2} \\
&\quad \times r_0^3 u^{-3} \mathrm{d}u \mathrm{d}r_0 \\
&= p_c(2\pi\lambda)^2 \int_0^1 \int_0^\infty e^{-\lambda\pi\left[p_c(1+p_a\rho(\theta_2 u^\alpha,\alpha))u^{-2}+(1-p_c)(1+(1-p_a)\rho(\theta_2,\alpha))\right] r_0^2} \\
&\quad \times r_0^3 \mathrm{d}r_0 u^{-3} \mathrm{d}u \\
&= p_c(2\pi\lambda)^2 \int_0^1 \frac{u^{-3}\mathrm{d}u}{2(\pi\lambda)^2(p_c(1+p_a\rho(\theta_2 u^\alpha,\alpha))u^{-2}+(1-p_c)(1+(1-p_a)\rho(\theta_2,\alpha)))^2} \\
&= p_c \int_0^1 \frac{\mathrm{d}x}{\left(p_c(1+p_a\rho(\theta_2 x^{\frac{\alpha}{2}},\alpha))+(1-p_c)(1+(1-p_a)\rho(\theta_2,\alpha))x\right)^2}.
\end{aligned} \tag{62}$$

The expressions of $\mathcal{M}_i, i = 2, 3$ and $\mathcal{Q}_j, j = 1, 2, 3$ can be obtained following the same steps as the one used for $\mathcal{M}_1$, by computing

$$\mathcal{M}_2 = \mathbb{E}_{T_1,R_0}\left[\mathcal{L}_{I_2}(\theta_2 T_1^\alpha)\right], \tag{63}$$

$$\mathcal{M}_3 = -\mathbb{E}_{T_1,R_0}\left[\mathcal{L}_{I_2}(\theta_2 R_0^\alpha)\mathcal{L}_{I_2}(\theta_2 T_1^\alpha)\right], \tag{64}$$

$$\mathcal{Q}_1 = \mathbb{E}_{T_1,R_0}\left[\mathcal{L}_{I_2}(\theta_2 R_0^\alpha)\mathcal{L}_{I_{0,1}}(\theta_1 R_0^\alpha)\right], \tag{65}$$

$$\mathcal{Q}_2 = \mathbb{E}_{T_1,R_0}\left[\mathcal{L}_{I_2}(\theta_2 T_1^\alpha)\mathcal{L}_{I_{0,1}}(\theta_1 R_0^\alpha)\right], \tag{66}$$

$$\mathcal{Q}_3 = -\mathbb{E}_{T_1,R_0}\left[\mathcal{L}_{I_2}(\theta_2 R_0^\alpha)\mathcal{L}_{I_2}(\theta_2 T_1^\alpha)\mathcal{L}_{I_{0,1}}(\theta_1 R_0^\alpha)\right], \tag{67}$$

and the proof is complete.

Abbreviations

BS	Base station
BWP	Bandwidth partitioning
i.i.e.d.	Independent and identically exponentially distributed
OPS	Optimal point selection
PPP	Poisson point process
RB	Resource block

SE	Spectral efficiency
SFR	Soft frequency reuse
SIR	Signal-to-interference ratio

Acknowledgements
Not applicable.

Author contributions
The authors have contributed jointly to the manuscript. All authors read and approved the final manuscript.

Funding
This work has been partially funded by the ANR project ARBURST under the Grant number ANR-16-CE25-0001.

Availability of data and materials
Not applicable.

Declarations

Ethics approval and consent to participate
Not applicable.

Consent for publication
Yes.

Competing interests
The authors declare that they have no competing interests.

Received: 28 March 2022 Accepted: 11 October 2022
Published online: 27 October 2022

References

1. M. Kamel, W. Hamouda, A. Youssef, Ultra-dense networks: a survey. IEEE Commun. Surv. Tutor. **16**, 2522–2545 (2018)
2. J. Yoon, G. Hwang, Distance-based inter-cell interference coordination in small cell networks: stochastic geometry modeling and analysis. IEEE Trans. Wirel. Commun. **17**, 4089–4103 (2018)
3. K. Feng, M. Haenggi, A location-dependent base station cooperation scheme for cellular networks. IEEE Trans. Commun. **67**, 6415–6426 (2019)
4. S.M. Yu, S.-L. Kim, Downlink capacity and base station density in cellular networks, in *11th International Symposium and Workshops on Modeling and Optimization in Mobile, Ad hoc and Wireless Networks (WiOpt)*, (2013), pp. 119–124
5. P.D. Mankar, H.S. Dhillon, Downlink analysis of noma-enabled cellular networks with 3g pp-inspired user ranking. IEEE Trans. Wirel. Commun. **19**, 3796–3811 (2020)
6. K.S. Ali, M. Haenggi, H. ElSawy, A. Chaaban, M.-S. Alouini, Downlink non-orthogonal multiple access (noma) in Poisson networks. IEEE Trans. Commun. **19**, 1613–1628 (2018)
7. P.D. Mankar, G. Das, S.S. Pathak, Load-aware performance analysis of cell center/edge users in random hetnets. IEEE Trans. Veh. Technol. **67**, 2476–2490 (2017)
8. C. Skouroumounis, C. Psomas, I. Krikidis, Heterogeneous fd-mm-wave cellular networks with cell center/edge users. IEEE Trans. Commun. **67**, 791–806 (2018)
9. H. Wang, K. Huang, T.A. Tsiftsis, Base station cooperation in millimeter wave cellular networks: performance enhancement of cell-edge users. IEEE Trans. Wirel. Commun. **66**, 5124–5139 (2018)
10. T.D. Novlan, R.K. Ganti, A. Ghosh, J.G. Andrews, Analytical evaluation of fractional frequency reuse for ofdma cellular networks. IEEE Trans. Wirel. Commun. **10**, 4294–4305 (2011)
11. H. Zhuang, T. Ohtsuki, A model based on poisson point process for analyzing mimo heterogeneous networks utilizing fractional frequency reuse. IEEE Trans. Commun. **13**, 6839–6850 (2018)
12. M. Mardani, P. Mary, J.-Y. Baudais, A tractable model for coverage in non-full interference cellular networks with cell center/edge users, in *IEEE International Workshop on Signal Processing Advances in Wireless Communications, Atlanta, Georgie, USA (virtual)*, (2020), pp. 1–5
13. F. Dominique, C.G. Gerlach, N. Gopalakrishnan, A. Rao, J.P. Seymour, R. Soni, A. Stolyar, H. Viswanathan, C. Weaver, A. Weber, Self-organizing interference management for lte. Bell Labs Tech. J. **15**, 19–42 (2010)
14. C. Skouroumounis, C. Psomas, I. Krikidis, A hybrid cooperation scheme for sub-6 ghz/mmwave cellular networks. IEEE Commun. Lett. **24**, 1539–1543 (2020)
15. M.V. Mardani, P. Mary, J.-Y. Baudais, A user-centric frequency reuse in non-full interference cellular networks, in: *IEEE Global Communications Conference, Taipei, Taiwan (virtual)*, (2020), pp. 1–6
16. G. Nigam, P. Minero, M. Haenggi, Coordinated multipoint joint transmission in heterogeneous networkss. IEEE Trans. Commun. **62**, 4134–4146 (2014)
17. N. Lee, D. Morales-Jimenez, A. Lozano, R.W. Heath, Spectral efficiency of dynamic coordinated beamforming: a stochastic geometry approach. IEEE Trans. Wirel. Commun. **14**, 230–241 (2014)
18. C. Li, J. Zhang, M. Haenggi, K.B. Letaief, User-centric intercell interference nulling for downlink small cell networks. IEEE Trans. Commun. **63**, 1419–1431 (2015)
19. F. Baccelli, A. Giovanidis, A stochastic geometry framework for analyzing pairwise-cooperative cellular networks. IEEE Trans. Wirel. Commun. **14**, 794–808 (2015)

20. Y. Li, M. Xia, S. Aïssa, Coordinated multi-point transmission: a poisson-delaunay triangulation based approach. IEEE Trans. Wirel. Commun. **19**, 2946–2959 (2020)
21. H. Wang, X. Tao, P. Zhang, Adaptive modulation for dynamic point selection/dynamic point blanking. IEEE Commun. Lett. **19**, 343–346 (2015)
22. Q. Cui, X. Yu, Y. Wang, M. Haenggi, The sir meta distribution in poisson cellular networks with base station cooperation. IEEE Trans. Commun. **66**, 1234–1249 (2017)
23. V. Chandrasekhar, J.G. Andrews, Spectrum allocation in tiered cellular networks. IEEE Trans. Commun. **57**, 3059–3068 (2009)
24. F. Baccelli, S.S. Kalamkar, Bandwidth allocation and service differentiation in d2d wireless networks, in *IEEE INFOCOM 2020-IEEE Conference on Computer Communications*, (2020), pp. 2116–2125
25. S.S. Kalamkar, Reliability and local delay in wireless networks: Does bandwidth partitioning help? in *IEEE Global Communications Conference* (GLOBECOM), (2019), pp. 1–6
26. S. Timotheou, I. Krikidis, Fairness for non-orthogonal multiple access in 5g systems. IEEE Signal Process. Lett. **22**, 1647–1651 (2015)
27. Y. Sun, D.W.K. Ng, Z. Ding, R. Schober, Optimal joint power and subcarrier allocation for full-duplex multicarrier non-orthogonal multiple access systems. IEEE Trans. Commun. **65**, 1077–1091 (2017)
28. M. Alsenwi, N.H. Tran, M. Bennis, S.R. Pandey, A.K. Bairagi, C.S. Hong, Intelligent resource slicing for embb and urllc coexistence in 5g and beyond: a deep reinforcement learning based approach. IEEE Trans. Wirel. Commun. **20**, 4585–4600 (2021)
29. K.S. Rao, V. Lakshminarayanan, *Generalized hypergeometric functions*. (IOP Publishing, 2018)
30. M. Haenggi, User point processes in cellular networks. IEEE Wirel. Commun. Lett. **6**, 258–261 (2017)
31. J.G. Andrews, F. Baccelli, R.K. Ganti, A tractable approach to coverage and rate in cellular networks. IEEE Trans. Commun. **59**, 3122–3134 (2011)
32. M. Sawahashi, Y. Kishiyama, A. Morimoto, D. Nishikawa, M. Tanno, Coordinated multipoint transmission/reception techniques for lte-advanced [coordinated and distributed mimo]. IEEE Wirel. Commun. **17**, 26–34 (2010)
33. S.N. Chiu, D. Stoyan, W.S. Kendall, J. Mecke, *Stochastic Geometry and Its Applications*. (John Wiley & Sons, Wiley Series in Probability and Statistics, 2013)
34. J.-Y. Huang, H.-F. Lu, Achieving large sum rate and good fairness in miso broadcast communication. IEEE Trans. Vehic. Technol. **68**, 5684–5695 (2019)
35. O. Mihatsch, R. Neuneier, Risk-sensitive reinforcement learning. Mach. Learn. **49**, 267–290 (2002)
36. H.M. Markowitz, G.P. Todd, *Mean-variance Analysis in Portfolio Choice and Capital Markets* (John Wiley & Sons, California, 2000)
37. D.P. Bertsekas, *Nonlinear Programming*, 2nd edn. (Athena Scientific, Greece, 1999)
38. C. Xing, Y. Jing, S. Wang, S. Ma, H.V. Poor, New viewpoint and algorithms for water-filling solutions in wireless communications. IEEE Trans. Signal Process. **68**, 1618–1634 (2020)
39. R.K. Jain, D.-M.W. Chiu, W.R. Hawe et al., A quantitative measure of fairness and discrimination. East. Res. Lab. **21**, 1–37 (1984)
40. T. Lan, D. Kao, M. Chiang, A. Sabharwal, An axiomatic theory of fairness in network resource allocation, in *IEEE International Workshop on Signal Processing Advances in Wireless Communications*, IEEE INFOCOM, (2010), pp. 1–17

Publisher's Note